Available online at www.sciencedirect.com
ScienceDirect
Journal of Power Sources 161 (2006) 1450–1457
JOURNAL OF POWER SOURCES
www.elsevier.com/locate/jpowsour

Photo-electrochemical hydrogen generation using band-gap modified nanotubular titanium oxide in solar light

K.S. Raja, M. Misra *, V.K. Mahajan, T. Gandhi, P. Pillai, S.K. Mohapatra

Metallurgical and Materials Engineering/M.S 388, University of Nevada, Reno 89557, USA

Received 8 March 2006; received in revised form 6 June 2006; accepted 7 June 2006
Available online 4 August 2006

Abstract

Anodization of Ti in acidified fluoride solution results in an ordered nanotubular titanium oxide surface. In this study, vertically oriented arrays of TiO_2 nanotubes were prepared by incorporating nitrate and phosphate species during the anodization process. These nanotubes were annealed at 650 °C in a carbonaceous atmosphere using a chemical vapor deposition (CVD) furnace for a brief period. The carbon-modified nanotubular TiO_2 produced a photo-current density of more than 2.75 mA cm^{-2} at 0.2 $V_{Ag/AgCl}$ under solar light illumination. This photo-current density corresponds to a hydrogen evolution rate of about 11 l h^{-1} using a photo-anode of 1 m^2 area. The enhanced hydrogen evolution behavior of carbon-modified nanotubular TiO_2 is highly reproducible and sustainable for long duration. Annealed (at 350 °C in nitrogen atmosphere) TiO_2 nanotubes showed improved photo-activity as compared to the as-anodized or thermally oxidized TiO_2 photo-anodes.

Keywords: Hydrogen generation; Titania nanotubes; Photo-electrochemical; Band-edges

1. Introduction

Among the available photo-sensitive materials, titanium dioxide is considered highly stable against photo-corrosion and is relatively inexpensive. Using a single crystal rutile wafer, Fujishima and Honda [1] first demonstrated photo-electrolysis of water by visible light. In a subsequent paper [2], the same authors used thermally or electrochemically oxidized Ti foils as anodes and observed an energy conversion efficiency of more than 0.4%. As the band-gap energy of TiO_2 is larger, only the UV portion of the solar spectrum can excite the photo-electrons. In order to make the TiO_2 more responsive to the natural solar spectrum, various approaches have been investigated. Among these approaches, band-gap modification and increasing the surface area by nanostructures are noteworthy.

With band-gap modification, Khan et al. [3] demonstrated a maximum photo-conversion efficiency of 8.35% using a chemically modified n-type TiO_2 film on Ti substrate. The higher photo-conversion efficiency was attributed to the lower band-gap energy (2.32 eV) of carbon doped n-$TiO_{2-x}C_x$ type film synthesized by combustion of the Ti metal sheet, which absorbed light at wavelengths below 535 nm. It should be noted that such a high photo-conversion efficiency reported by Khan et al. was not reproducible by others [4,5]. Band-gap narrowing was also observed in nitrogen doped TiO_2 nano-particles [6].

TiO_2 nanocrystalline anodes have been fabricated by various routes such as: coating a titania slurry onto conducting glass, [7] spray pyrolysis, and layer-by-layer colloidal coating on a glass substrate followed by calcinations at an appropriate temperature. These processes result in the formation of a 3-D network of interconnected nanoparticles. It was suggested that instead of the 3-D configuration of nanoparticles, fabrication of vertical standing nanowires of TiO_2 could improve the photo-conversion efficiency [8]. Anodization of a titanium metal substrate in acidified fluoride solution results in the formation of ordered arrays of vertically standing TiO_2 nanotubes [9–11].

Recently Grimes and co-workers [12] reported the photo-electrolysis properties of anodized titanium oxide nanotubes. These authors reported a photo-conversion efficiency of 6.8% with an array of anodized TiO_2 nanotubes having a 22 nm diameter, 34 nm wall thickness and were 224 nm long. In a subsequent publication, these authors reported 6 μm long TiO_2 nanotubes showing less than 0.4% efficiency for water photo-electrolysis using a simulated solar spectrum of light (AM 1.5) [13]. In

* Corresponding author. Fax: +1 775 784 1603.
E-mail address: misra@unr.edu (M. Misra).

0378-7753/$ – see front matter © 2006 Elsevier B.V. All rights reserved.
doi:10.1016/j.jpowsour.2006.06.044

these investigations, altering the wall thickness and the length of the nanotubes controlled the photo-electric properties. Schmuki and co-workers [14] investigated the effect of nitrogen doping on the TiO_2 nanotubes prepared by anodization in 1 M H_2SO_4 + 0.15 wt.% HF electrolyte. Nitrogen doping of TiO_2 after ammonia treatment at 600 °C, resulted in a photo-current density of 0.1 mA cm^{-2} at a bias potential of 0.5 $V_{Ag/AgCl}$ and about 0.37 mA cm^{-2} at 3.0 $V_{Ag/AgCl}$ in 0.1 M Na_2SO_4 electrolyte by irradiating with 450 nm light. Bard and co-workers [15] prepared $TiO_{2-x}C_x$ nanotubular arrays and reported more efficient water splitting under visible light illumination.

In this investigation, we have tried to combine both band-gap modification and ordered nanostructure approaches to enhance the photo-electrochemical properties of TiO_2. Incorporation of nitrate and phosphate species was carried out during anodization and the effect on photo-electrolysis was investigated. The effect of a carbon-modified nanotubular TiO_2 structure on the hydrogen generation behavior was also investigated. It should be noted that during water electrolysis, oxygen evolves on the TiO_2 surface and hydrogen evolves on the cathode. Enhanced photo-activity of the TiO_2 results in enhanced oxygen evolution on its surface and correspondingly hydrogen evolution increases at the cathode.

2. Experimental

Sixteen millimeter discs were punched from a stock of Ti foil (0.2 mm thick, 99.9% purity, ESPI-metals, Ashland, Oregon, USA) and secured in a PTFE holder exposing only 0.7 cm^2 area to the electrolyte. Nanotubular TiO_2 arrays were formed by anodization of the Ti foils in one of the following electrolyte solutions:

(1) 0.5 M H_3PO_4 + 0.14 M NaF (pH 2.0), referred as phosphate solution;
(2) 0.5 M H_3PO_4 + 0.14 M NaF + 0.05–1.0 M $NaNO_3$ (pH 2.0);
(3) 0.5–1.0 M $NaNO_3$ + 0.14 M NaF (pH 3.8–5.0 adjusted with addition of HNO_3), referred as nitrate solution.

A two-electrode configuration was used for anodization. A flag shaped Pt electrode served as the cathode. The anodization was carried out at 20 V. Initially the potential was ramped at a rate of 0.1 V s^{-1} from free corrosion potential to the final anodization potential of 20 V. The anodization current was monitored continuously. After an initial transient, the current reached a steady state value of about 1.1–1.4 mA cm^{-2}. The anodization was continued for 20 min after reaching the above current plateau value in lower pH electrolytes. Anodization was carried out for a longer time, of the order of 3–7 h, in the higher pH solutions. The total anodization time for the pH 2 solution was about 50 min and in other pH solutions the time varied from 1 to 6 h. The anodization was carried out at room temperature (~24 °C) with continuous stirring of the solution using a magnetic stirrer.

The anodized specimens were annealed in a nitrogen or hydrogen atmosphere at 350–500 °C for 1–6 h. In another set of experiments, the anodized specimens were heated in a chemical vapor deposition furnace at 650 °C for 5–20 min in a gas mixture of acetylene + argon + hydrogen with a typical flow rate of 20, 40 and 200 cm^3 min^{-1} respectively. Heat treatment of anodized specimens in a carbon containing gas mixture resulted

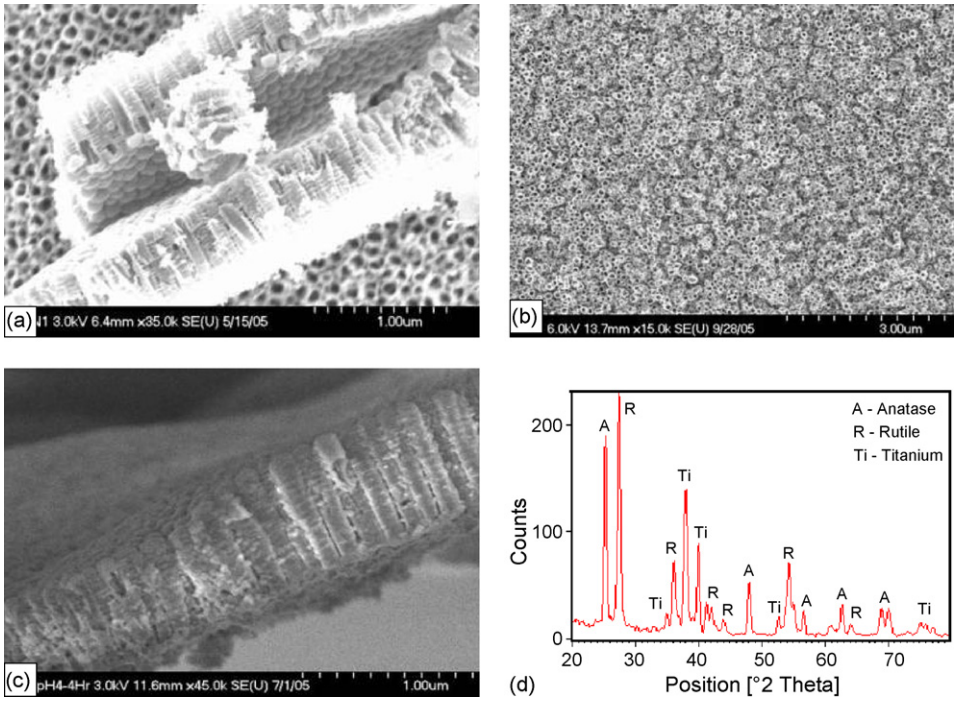

Fig. 1. Scanning electron microscopic images of anodized nanotubular TiO_2 surface layer: (a) anodized in 0.5 M H_3PO_4 + 0.1 M $NaNO_3$ + 0.14 M NaF at 20 V, 45 min; top surface morphology and cross sectional view of the oxide layer are seen. The oxide was mechanically cracked; (b) anodized in 0.5 M $NaNO_3$ + 0.14 M NaF (pH 4.0) at 20 V for 4 h; (c) side view showing the length of nanotubes as in condition (b); (d) XRD pattern of annealed nanotubes showing crystalline phases.

in incorporation of nanostructured–graphitized carbon into the nanotubes of the TiO_2 arrays. The electronic band-gap values of the TiO_2 samples were measured from the optical absorption spectra using a UV–VIS spectrometer (Model: UV-2401 PC, Shimadzu Corporation, Kyoto, Japan). Further characterization of the TiO_2 nanotubes was carried out by high-resolution X-ray photo-electron spectroscopy (XPS) and Mott–Schottky analysis. The Mott–Schottky analysis was carried out by conducting a standard electrochemical impedance spectroscopy at 3000 Hz in 1 M NaOH solution by scanning the potential from positive to negative direction in steps of 50 mV s^{-1}.

Photo-electrochemical studies were carried out in a glass cell having separate compartments for the photo-anode (nanotubular TiO_2 specimen) and cathode (platinum foil). The compartments were connected by a fine porous glass frit. A reference electrode (Ag/AgCl) was placed closer to the anode using a salt bridge (saturated KCl)-Luggin probe capillary. The cell was provided with a 60 mm diameter quartz window for light incidence. The electrolyte used was 1 M NaOH. A computer-controlled potentiostat (Model: SI 1286, Schlumberger, Farnborough, England) was employed to control the potential and record the photo-current. A 300 W solar simulator (Model: 69911, Newport-Oriel Instruments, Stratford, CT, USA) was used as a light source. The light at 300 W power level was passed through an AM 1.5 Global filter. Photo electrochemical studies were carried out in different combinations of band pass filters: (1) AM 1.5 filter, (2) AM 1.5 + UV filter (250–400 nm, Edmund Optics, U330, center wave length 330 nm and FWHM: 140 nm) and (3) AM 1.5 + visible band pass filter (Edmund Optics, VG-6, center wave length 520 nm and FWHM: 92 nm). The intensity of the light was measured by a radiant power and energy meter (Model 70260, Newport Corporation, Stratford, CT, USA) and a thermopile sensor (Model: 70268, Newport). The incident light intensities without any corrections were 174, 81 and 66 mW cm^{-2} with AM 1.5 filter, AM 1.5 + UV filters, and AM 1.5 + VIS filters respectively. The samples were anodically polarized at a scan rate of 5 mV s^{-1} under illumination and the photo-current was recorded. The potential of photo-anode and cathode also was recorded for calculation of photo-conversion efficiency.

3. Results and discussion

Fig. 1(a) shows the nanotubular TiO_2 arrays in the as-anodized condition (anodized in 0.5 M H_3PO_4 + 0.1 M $NaNO_3$ + 0.14 M NaF at 20 V, for 45 min). Fig. 1(b and c) show the nanotubular arrays after anodization in 0.5 M $NaNO_3$ + 0.14 M NaF (pH 4.0 by adding HNO_3) solution at 20 V for 4 h. Low temperature annealing did not change the nanotubular structure (not shown in figure). The tubes were about 400–800 nm long and showed a diameter in the range of 60–100 nm. Increase in pH of the solution and anodization time increased the length of the nanotubes. Annealing at 350 °C resulted in transformation of amorphous structure of the TiO_2 to crystalline anatase and rutile phases as indicated in Fig. 1(d).

Fig. 2(a) shows the nanotubular TiO_2 arrays annealed in an acetylene + hydrogen gas mixture at 650 °C for 5 min. A very thin layer of carbon could be observed. Increasing the exposure time in the carbonaceous environment resulted in growth of carbon nanostructures within the TiO_2 nanotubes. The amount of carbon incorporation increased with increase in treatment time and the color of the samples also changed from light-gray to dark-gray. Longer than a 20 min treatment resulted in complete coverage of the TiO_2 with the carbon nanocones as illustrated in Fig. 2(b).

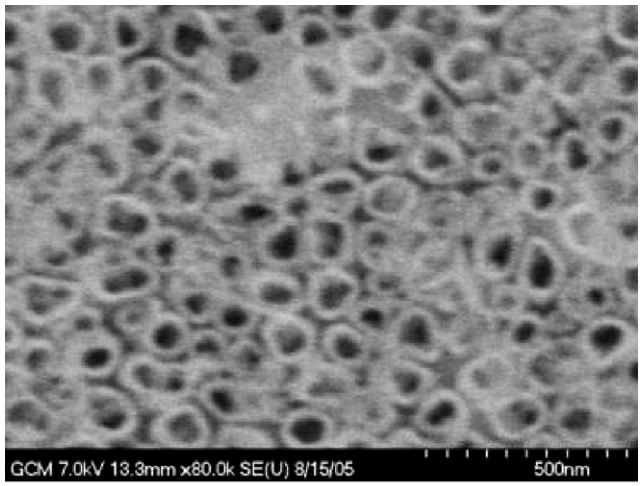

Fig. 2. Surface morphology of nanotubular TiO_2 after annealing at 650 °C in acetylene + hydrogen gas mixture: (a) for 5 min and (b) for 20 min. Longer exposure time resulted in growth of carbon nano-structures inside the TiO_2 nanotubes.

Fig. 3(a) shows the optical absorption spectra of nanotubular TiO_2 arrays anodized in nitrate solution at different heat-treated conditions. Fig. 3(b) is the absorption spectra of samples anodized in phosphate solution. The annealed specimen (annealed at 350 °C for 6 h) showed a 30 nm red shift of absorption peak as compared to that of as-anodized sample. Annealing either in an inert (N_2) or in a reducing (H_2) atmosphere resulted in similar optical absorption characteristics. It is envisaged that anodization in nitrate containing solutions could result in adsorbed nitrogen species on the nanotubular structure and the creation of surface states. Sakthivel and Kisch reported narrowing of the band-gap of nitrogen doped titania prepared by the hydrolysis of titanium tetrachloride in nitrogen containing

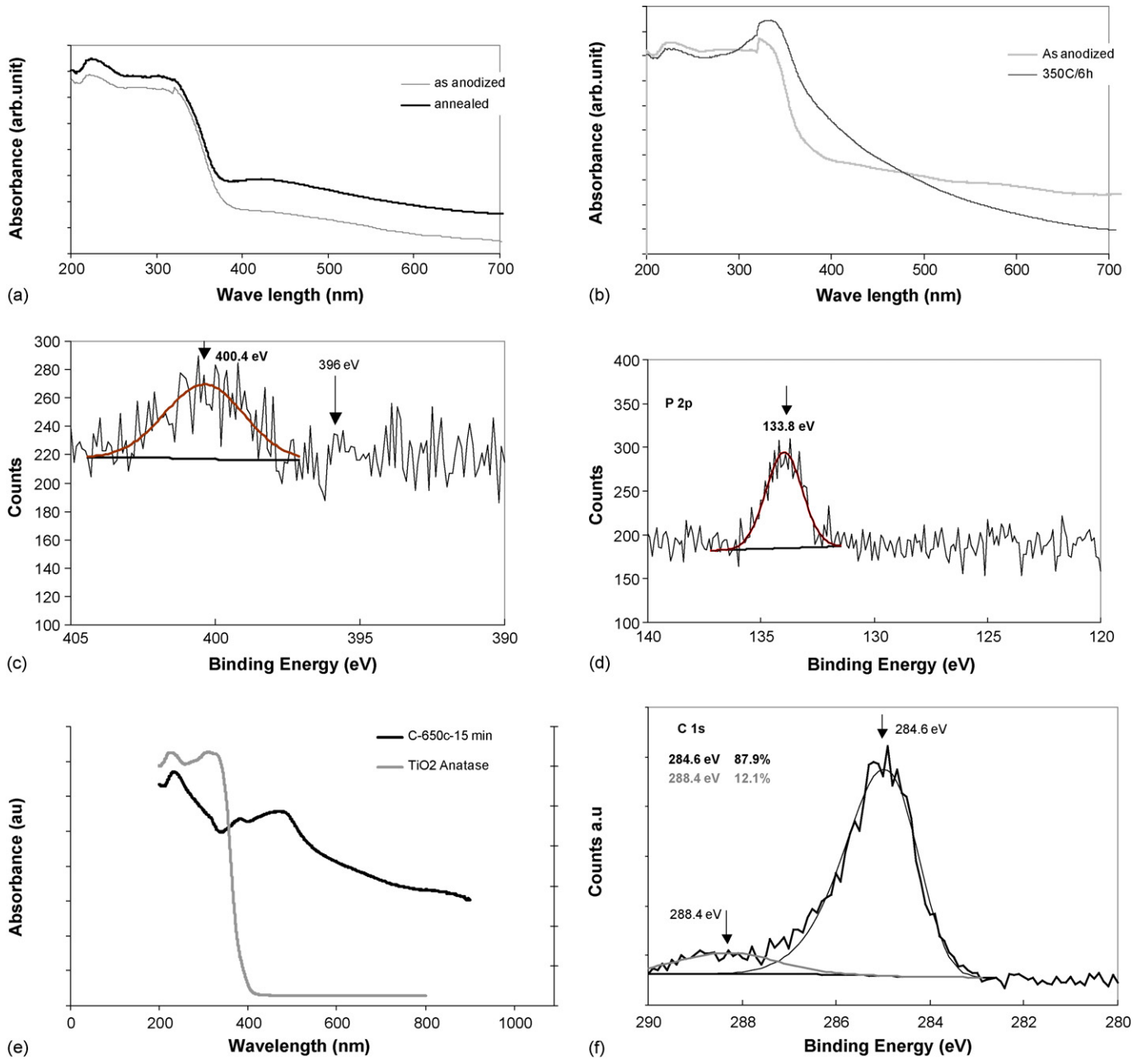

Fig. 3. (a) and (b). Optical absorbance spectra of TiO_2 ordered nanotubular samples: (a) anodized in 0.5 M $NaNO_3$ + 0.14 M NaF solution (pH 4) and (b) anodized in 0.5 M H_3PO_4 + 0.14 M NaF. Annealing was carried out at 350 °C in nitrogen atmosphere for 6 h. (c) N 1s XPS spectrum of the TiO_2 nanotubes anodized in nitrate solution and annealed in nitrogen atmosphere. Molecularly chemisorbed N_2 peak at 400 eV is observed. Peak at 396 eV associated with Ti—N bonding is not observed. (d) P 2p XPS spectrum of the TiO_2 nanotubular sample anodized in phosphate solution. The peak at 133.8 eV indicates incorporation of phosphate-type species in the TiO_2 lattice. (e) Absorbance spectra of nanotubular TiO_2 annealed in acetylene + hydrogen gas mixture at 650 °C for 10 min in comparison with a standard anatase powder absorbance. (f) C 1s XPS spectrum of carbon-modified TiO_2 nanotubes. The peak at 284.6 eV is associated with adventitious elemental carbon and the peak at 288.4 eV is attributed to the carbonate type species.

base, followed by calcinations in air at 400 °C [16]. The presence of hyponitrite was accounted for the observed surface states in their titania sample. Asahi et al. [6] also observed doping of nitrogen in titania when the TiO_2 powder was heated in an ammonia + argon gas mixture at 550–600 °C. However, direct evidence for the incorporation of nitrogen into the TiO_2 lattice could not be obtained from the XPS results. Fig. 3(c) shows a typical N 1s XPS spectrum of the TiO_2 nanotubular sample anodized in nitrate solution and annealed in nitrogen atmosphere. Only a molecularly chemisorbed nitrogen peak at 400 eV was observed. The peak at 396 eV was associated with Ti–N bonding and was not predominant.

It was observed that samples anodized in phosphate solutions showed relatively better optical absorption as compared to the samples anodized in nitrate solutions. It is envisaged that anodization in an 0.5 M H_3PO_4 + 0.14 M NaF solution results in adsorption of phosphate ions at the outer walls of the TiO_2 nanotubes and subsequent annealing in low oxygen pressure

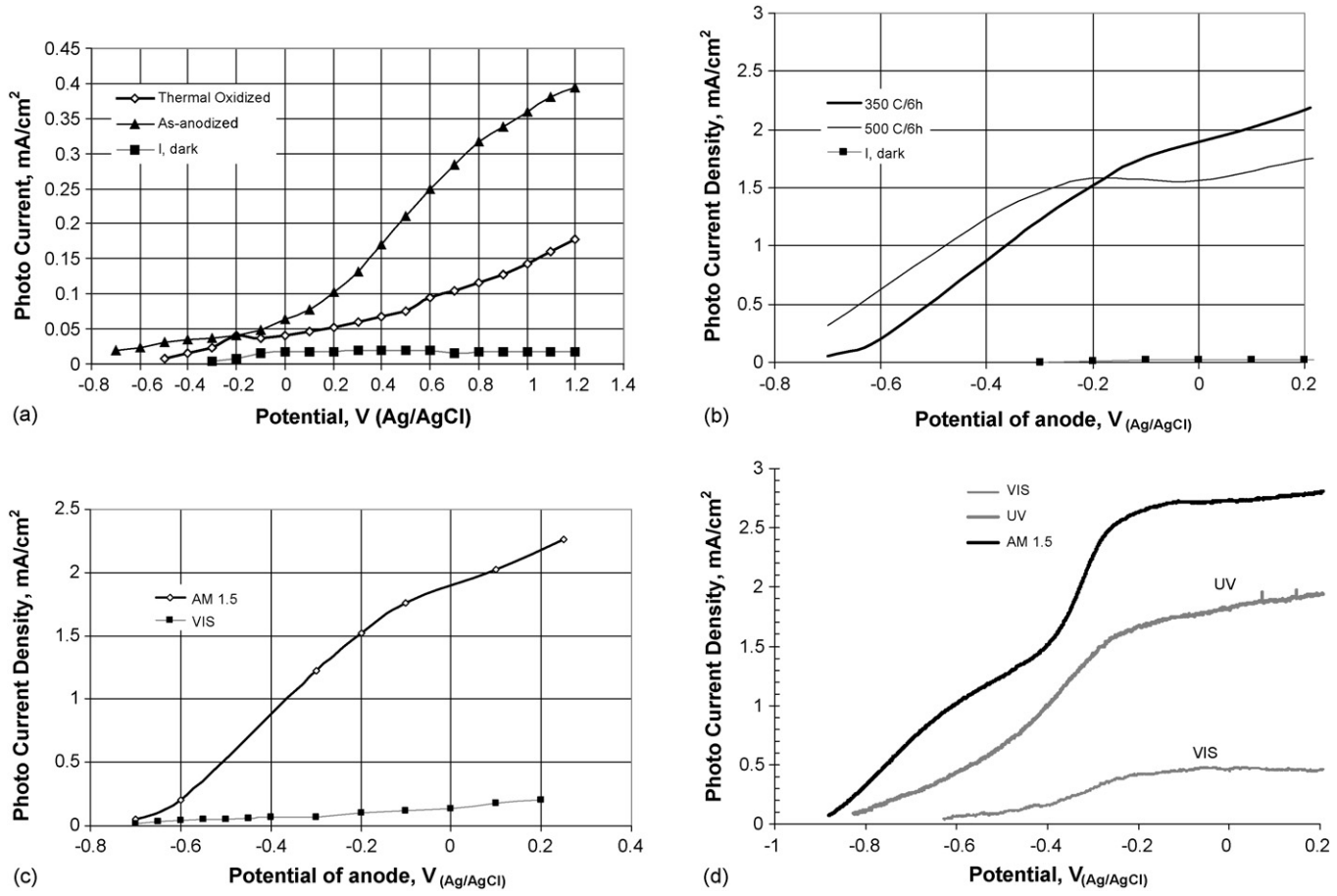

Fig. 4. (a) Photo-current generated by nanotubular TiO_2 in as anodized condition (anodized in phosphate solution) in comparison with Ti foil thermally oxidized at 850 °C for 15 min in CO_2 atmosphere. The electrolyte was 1 M NaOH. Samples were illuminated simulating AM 1.5 condition. (b) Photo-current generated by nanotubular TiO_2 in N_2-annealed condition (anodized in phosphate solution). The electrolyte was 1 M NaOH. Samples were illuminated simulating AM 1.5 condition. (c) Photo-current–potential characteristics of the annealed TiO_2 nanotubular array in the AM 1.5 light and visible light without UV spectrum (VIS-with center wavelength at 520 nm and FWHM of 92 nm). (d) Photo-current–potential characteristics of the carbon-modified (treated at 650 °C for 5 min) TiO_2 nanotubular array in the AM 1.5 light, UV light (CWL: 330, FWHM: 140 nm) and visible light without UV spectrum (VIS-with center wavelength at 520 nm and FWHM of 92 nm).

could cause diffusion of phosphorous species in the TiO_2 lattice creating a sub-band gap or surface states. Fig. 3(d) shows the high-resolution P 2p XPS spectrum and the peak at 133.8 eV indicates incorporation of the phosphorous species in the TiO_2 nanotubes [17].

Fig. 3(e) shows the absorption spectra of samples modified by the deposition of nano-structured carbon (referred as carbon-modified samples). The presence of carbon resulted in light absorption in the visible range of wavelengths in addition to the regular absorption of titanium oxide. These results are in agreement with other reported work in the literature [18,19]. The major differences between this work and the other reported work are the form of carbon present and morphology of the TiO_2 supporting the carbon species. Carbon doped titania prepared by a sol–gel method was considered to have carbon in the form of carbonate [18,19]. Khan et al. [3] reported formation of carbon-modified n-TiO_2 film on Ti foil by natural gas flame pyrolysis. The flame-made TiO_2 was considered porous and contained about 15 at% carbon. These carbon atoms were considered to be a substitute for lattice oxygen of TiO_2. In this work, TiO_2 was present as ordered nanotubes as compared with nanoparticles or thin oxide layers reported in the literature and the carbon was present as a carbon nano-structure forming a composite material. The adsorption at visible wavelengths increased with increase in the carbonaceous treatment time. The width of the additional shoulder of the major TiO_2 absorbance peak decreased with increase in the heat-treatment time of the samples in the carbon-containing gas atmosphere. Fig. 3(f) shows a typical C 1s XPS spectrum of the carbon-modified TiO_2 nanotubular sample. The peak at 288.4 eV could be attributed to the carbonate type species incorporated in the nanotubes during thermal treatment in the acetylene gas mixture. This observation is similar to the results of other investigators [18,19].

Fig. 4(a) shows the results of electrochemical hydrogen generated in terms of photo-current during illumination for the as-anodized and annealed TiO_2 samples using simulated 1-sun light intensity. The dark current density is always less than 10 $\mu A\,cm^{-2}$ for all the samples under anodically polarized conditions. Under illumination and at applied potentials, the photo-current density increased with increase in potential

for as-anodized samples. For comparison, photo-current data of the thermally oxidized Ti foil has been included. The Ti foil was oxidized at 850 °C for 15 min in a CO_2 atmosphere. As expected, thermally oxidized samples did not generate significant photo-current. As-anodized TiO_2 nanotubes showed relatively higher photo-currents. In the as-anodized condition, the nanotubes of TiO_2 are considered to be amorphous. Mor et al. [11,13] reported less than 0.08 mA cm^{-2} photo-current density at any applied potential condition for amorphous samples anodized in 0.5 wt.% HF + acetic acid mixture. In this investigation, as-anodized samples showed an increasing trend of photo-current with increase in applied potential (as against no-effect of applied potential in other studies [11,13]) and more than 0.3 mA cm^{-2} at higher applied potentials. The increased photo-activity of the sample in the amorphous condition as compared to that of previously reported samples can be attributed to the surface modification effect of phosphorous species in the nanotubes. Asahi et al. [6] calculated density of states (DOS) for doping of carbon and phosphorous in the anatase TiO_2 crystal and considered that the states introduced by these substitutions were too deep for overlapping with TiO_2 band gaps. However, increased photo-activity of the carbon-doped TiO_2 nanotubes has been well documented. Li et al. [19] argued that the observed increase in the photo-activity of the carbon doped TiO_2 did not contradict the theoretical prediction of Asahi et al. [6], as the carbon was present as carbonate, not as a substituted oxygen sub-lattice. Similarly, incorporation of phosphorous species also can be considered to increase the photo-activity of TiO_2. Further, it should be noted that increased photo-activity was observed even in amorphous TiO_2. Almost similar photo-current behavior was observed for samples anodized in nitrate solutions.

Fig. 4(b) illustrates the photo-electrochemical behavior of TiO_2 nanotubes annealed at 350 and 500 °C. In line with the optical absorption characteristics, both the annealed conditions showed almost similar photo-current behaviors at different external bias conditions. Fig. 4(c) shows the photo-current–potential characteristics of the annealed phosphate containing TiO_2 nanotubes illuminated only in the visible light having a center wavelength (CWL) at 520 nm and FWHM of 92 nm. In the absence of the UV component, the photo-activity of the TiO_2 nanotubes decreased considerably. The photo-current density at a bias potential of 0.2 V was about 0.2 mA cm^{-2}. It should be noted this value was higher than the value reported for nitrogen-doped nanotubes with a similar bias condition [14].

Fig. 4(d) shows the photo-current results of carbon-modified TiO_2 samples as a function of the applied potential. When the UV component was filtered out from the solar light, the composite electrode showed a photo-current density of 0.45 mA cm^{-2} under the applied anodic potentials. The photo-current density measured in the visible light (without UV) illumination was similar to that reported by Bard and co-workers [15] for the $TiO_{2-x}C_x$ material prepared by a different route. A composite electrode of carbon-modified nanotubular TiO_2 showed a photo-current density of 2.75 mA cm^{-2} under sunlight illumination at more anodic potentials. This photo-current density corresponds to a hydrogen evolution rate of 111 h^{-1} on a photo-anode with 1 m^2 area. The gases evolved in the cathode and anode compartments were analyzed separately using gas chromatography and the ratio of hydrogen to oxygen was 2:1, indicating that carbon in the carbon-modified TiO_2 sample was stable. Further, the hydrogen generation was stable for more than 72 h. The long-term test was interrupted because of the limited life of the lamp. It has been reported that the photo-current density decreased with increase in surface area of nanostructured TiO_2 prepared by the sol–gel route [20]. In this present study, carbon-modified TiO_2 nanotubular samples with 0.5–16.0-cm^2 geometric surface areas were evaluated and the photo-current density remained constant irrespective of the surface area of the anode.

The photo-electrochemical behavior of the samples is in line with the optical absorbance results, even though it is established that band-gap modification alone does not result in increased photo-activity [21]. Recently Yu et al. [22] reported enhanced photo-catalytic activity of mesoporous TiO_2-carbon nanotube (CNT) composite by investigating the degradation of acetone. In addition to the increased surface area by CNT, suppression of the recombination of electron–hole pairs by CNT was attributed to the increased photo-activity. However, addition of excessive CNTs was found to be detrimental as it completely shielded the titania from absorbing light [22]. Almost similar result was observed in this investigation also. Larger coverage of carbon nanostructure resulted in decreased photo-activity. The samples annealed at 650 °C for 5 min did not show presence of well-defined carbon nano-structures. However, enhanced photo-current was observed on these samples as compared to the samples treated for longer than 15 min in the carbonaceous atmosphere. Further, carbon-modified samples showed better photo-electrochemical behavior than annealed samples in the inert atmosphere. This improved behavior could be attributed to possibly two reasons, viz., (1) band-gap states introduced by carbon and (2) presence of trivalent Ti interstitials and oxygen vacancy states introduced by the reducing environments.

Alternately it is possible that carbon is not directly involved as band-gap states leading to decrease in the band gap; but the (reducing) environment during annealing in the presence of carbonaceous species resulted in reduction of Ti^{4+} to Ti^{3+} and formed oxygen vacancy states. In this study, enhanced absorption in the visible wavelength suggests that carbon modification resulted in local band-gap states. High-resolution XPS studies carried out on the nitrogen/hydrogen annealed samples and carbon-modified TiO_2 nanotubular samples suggested the presence of Ti^{3+} species. The presence of Ti^{3+} cations in the TiO_2 should be associated with oxygen vacancies in order to maintain electro-neutrality. Fig. 5(a) illustrates the Ti 2p XPS spectrum of nitrogen annealed TiO_2 nanotubular specimen. The 458.3 eV is attributed to the Ti^{4+} ions in the TiO_2 lattice [23]. The asymmetric nature of the peak indicates that the Ti^{4+} ions are not fully coordinated and a faint shoulder at 456.7 eV indicates the presence of Ti^{3+} ions [24]. These results suggest the presence of oxygen vacancies. Similar results were observed on the hydrogen annealed and carbon-modified TiO_2 nanotubular specimens. The TiO_2 nanotubes are considered as n-type semiconductors. Mott–Schottky results also show n-type behavior, as shown in Fig. 5(b) and (c). If the oxygen vacancies are produced during annealing in nitrogen or hydrogen atmosphere, the charge carrier

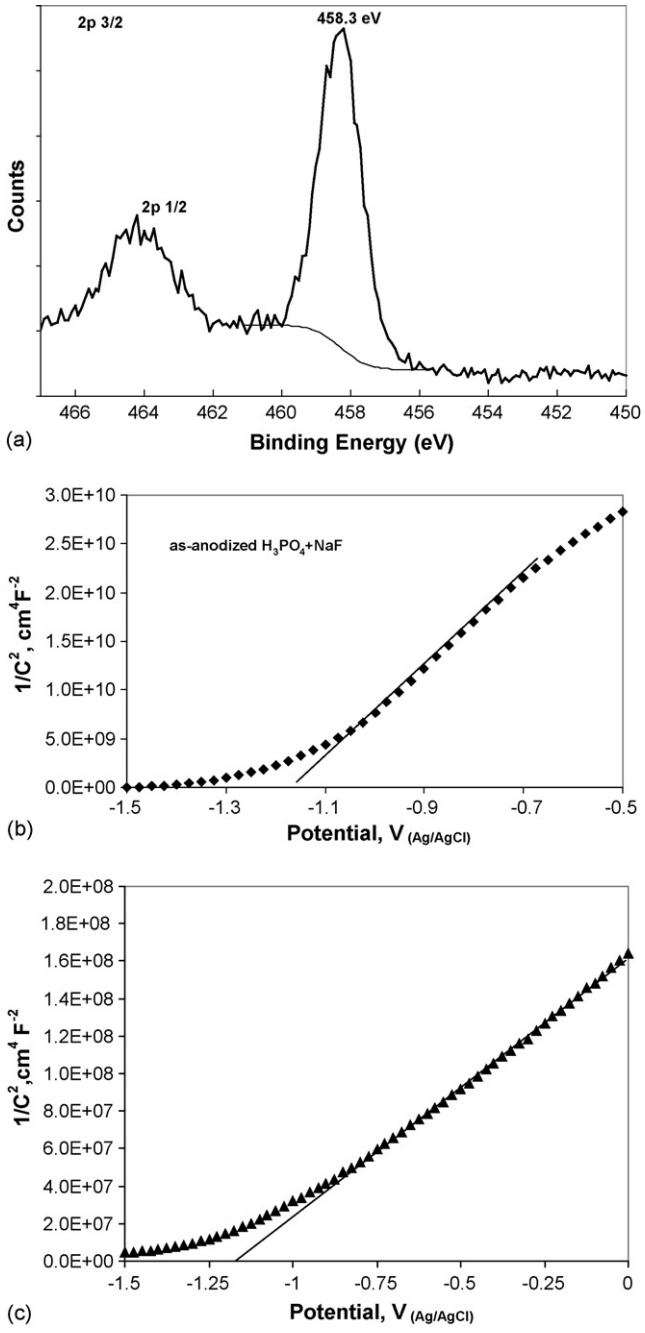

Fig. 5. (a) Ti 2p XPS spectrum of nitrogen annealed TiO_2 nanotubular specimen. The 458.3 eV is associated with Ti^{4+} ions. Asymmetric nature of the peak indicates that Ti^{4+} ions are not fully coordinated and a faint shoulder at 456.7 eV indicates presence of Ti^{3+} ions. (b) Mott–Schottky plot of as-anodized TiO_2 nanotubular specimen in 1 M NaOH solution at room temperature. (c) Mott–Schottky plot of TiO_2 nanotubular specimen, annealed in nitrogen at 350 °C for 6 h. Interfacial capacitance was measured in 1 M NaOH solution at room temperature.

density would increase. The charge carrier density can be calculated from the slope of the linear portion of the Mott–Schottky plots [25,26]. The plots in Fig. 5(b and c) are based on the geometric areas of the samples. The charge density of the as-anodized TiO_2 nanotubes based on the theoretical surface area was 1.1×10^{17} cm^{-3} and the annealed sample showed a charge density of 1.9×10^{19} cm^{-3}. The increase in charge density could be attributed to the oxygen vacancies introduced after annealing in the inert or reducing environments. However, the flat band potentials did not change significantly.

From the UV–VIS photo-spectroscopic results, it was evident that annealed and carbon-modified samples showed absorption at longer wavelengths because of the oxygen vacancy states introduced below the conduction band edge. However, for photo-generation of hydrogen, an anodic bias was required indicating that the Fermi level of the cathode was not sufficiently higher than the H_2/H_2O energy level for instantaneous electron transfer using visible light alone.

4. Conclusions

Anodization of Ti in phosphate or nitrate containing fluoride solutions resulted in ordered TiO_2 nanotubes that incorporated P or N species. Annealing the nanotubes in a nitrogen atmosphere at 350 °C resulted in increased photo-activity.

Annealing the TiO_2 nanotubes in a carbonaceous gas mixture at 650 °C for 5–20 min resulted in band-gap states due to the introduction of oxygen vacancies. The composite photo-anode showed enhanced photo-current at applied potentials in 1 M NaOH electrolyte under AM 1.5 light illumination.

Acknowledgements

This work was sponsored by U.S. Department of Energy through DOE Grant No.: DE-FC52-98NV13492 and DE-FG36-06GO86066. The authors gratefully acknowledge the financial support of DOE. The authors thank Mr. Gautam Priyadharshan and Dr. Mo Ahmedian for their assistance in the experimental work.

References

[1] A. Fujishima, K. Honda, Nature 238 (1972) 37–38.
[2] A. Fujishima, K. Kohayakawa, K. Honda, J. Electrochem. Soc. 122 (1975) 1487–1489.
[3] S.U.M. Khan, M. Al-Shahry, W.B. Ingel Jr., Science 297 (2002) 2243–2245.
[4] C. Hagglund, M. Gratzel, B. Kasemo, Science 301 (2003) 1673b.
[5] K. Noworyta, J. Augustynski, J. Electrochem, Solid State Lett. 7 (2004) E31–E33.
[6] R. Asahi, T. Morikawa, T. Ohwaki, K. Aoki, Y. Taga, Science 293 (2001) 269–271.
[7] J. van de Lagemaat, N.-G. Park, A.J. Frank, J. Phys. Chem. B 104 (2000) 2044–2052.
[8] S.U.M. Khan, T. Sultana, Solar Energy Mater. Solar Cells 76 (2003) 211–221.
[9] K.S. Raja, M. Misra, K. Paramguru, Mater. Lett. 59 (2005) 2137–2141.
[10] K.S. Raja, M. Misra, K. Paramguru, Electrochim. Acta 51 (2005) 154–165.
[11] G.K. Mor, O.K. Vargheese, M. Paulose, N. Mukherjee, C.A. Grimes, J. Mater. Res. 18 (2003) 2588–2591.
[12] G.K. Mor, K. Shankar, M. Paulose, O.K. Varghese, C.A. Grimes, Nanoletters 5 (2005) 191–195.
[13] M. Paulose, G.K. Mor, O.K. Varghese, K. Shankar, C.A. Grimes, J. Photochem. Photobiol. A: Chem. 178 (2006) 8–15.
[14] R.P. Vitello, J.M. Macak, A. Ghicov, H. Tsuchiya, L.F.P. Dick, P. Schmuki, Electrochem. Commun. 8 (2006) 544–548.
[15] J.H. Park, S. Kim, A.J. Bard, Nanoletters 6 (2006) 24–28.
[16] S. Sakthivel, H. Kisch, Chem. Phys. Chem. 4 (2003) 487–490.

[17] A. Ghicov, H. Tsuchiya, J. Macak, P. Schmuki, Electrochem. Commun. 7 (2005) 505–509.
[18] S. Sakthivel, H. Kisch, Angew. Chem. Int. Ed. 42 (2003) 4908–4911.
[19] Y. Li, D.-S. Hwang, N.H. Lee, S.-J. Kim, Chem. Phys. Lett. 404 (2005) 25–29.
[20] P.R. Mishra, P.K. Shukla, A.K. Singh, O.N. Srivatsava, Int. J. Hydrogen Energy 28 (2003) 1089–1094.
[21] J. Nowotny, C.C. Sorrell, T. Bak, L.R. Sheppard, Solar Energy 78 (2005) 593–602.
[22] Y. Yu, J.C. Yu, J.G. Yu, Y.C. Kwok, Y.K. Che, J.C. Zhao, L. Ding, P.K. Wong, Appl. Catal. A: Gen. 289 (2005) 186–196.
[23] C.E.B. Marino, P.A.P. Nascene, S.R. Biaggio, R.C. Rocha-Filho, N. Bocchi, Thin Solid Films 468 (2004) 109–112.
[24] F. Guillemot, M.C. Porte, C. Labrugere, Ch. Baquey, J. Colloid Interface Sci. 255 (2002) 75–78.
[25] J.E. Turner, M. Hendewerk, G.A. Somarjai, Chem. Phys. Lett. 105 (1984) 581–585.
[26] S.S. Kocha, J.A. Turner, A.J. Nozik, J. Electroanal. Chem. 367 (1994) 27–30.